

Electric Field Effect on the Thermal Decomposition and Co-Combustion of Straw Pellets with Peat

Inesa Barmina^a, Antons Kolmickovs^{a,*}, Raimonds Valdmanis^a, Maija Zake^a, Harijs Kalis^b, Uldis Strautins^b

^aInstitute of Physics, University of Latvia, 32 Miera str., Salaspils-1, LV-2169, Latvia

^bInstitute of Mathematics and Informatics, University of Latvia, 29 Raina blvd, Riga, LV-1459, Latvia
 kolmic@lu.lv

The main goal of the present study is to obtain a more effective utilization of wheat straw for energy production during a co-combustion with peat. For this purpose, an electric field was applied to the flame produced by the combustion of volatiles. This work combines experimental study and mathematical modelling of the processes developing during the co-combustion of straw pellets with peat pellets. The main gasification/combustion characteristics, the heat output from the device and the composition of the flue gas were analysed by varying separately the bias voltage of the axial electrode and the straw mass load in the mixture with intention to assess the electric field impact. A mathematical model of the electric field impact on the main combustion characteristics (flow velocity, flame temperature and composition) of co-combustion have been built within the MATLAB environment. The numerical simulation was performed for two dominant second order combustion reactions of CO and H₂ with account for the electric field effect on the displacement of equilibrium during the thermal decomposition of the biomass.

1. Introduction

With account of the EU clean energy targets (20-20-20) which prescribe that about 20 % of energy must be produced from renewable sources. There is a growing demand for wider use of fuels (agriculture residues) that need further application adjustment. With the aim to reduce the problems of straw utilization as a fuel (Olsson, 2006), the effects of the wheat straw co-combustion with different types of fuels on the main gasification/combustion characteristics were considered and analysed. The works of other authors have shown straw additive potential to improve the combustion characteristics (Veijonen et al., 2003) and ash formation (Nordgren et al., 2013). The results of previous research revealed that the main combustion characteristics – flame shape and size, can be controlled by the electric field. The electric field induced body force enhances the heat and mass transfer of the flame species in the field direction (ion wind effects) (Barmina et al., 2016a), and the field induced Lorentz force boosts up the flow vorticity with the enhanced air-fuel premixing (Barmina et al., 2016b). The combined experimental and mathematical study suggests that there should be many factors leading to unpredictable electric field effects on the flame characteristics, especially in the case of combustion of different fuel mixtures with the varying elemental and chemical composition. To assess the main factors determining the field effects on the main combustion characteristics and to give an insight into the processes developing at co-combustion of fuel mixtures of different elemental and chemical composition a fundamental study is required. The development of thermal decomposition of the main biomass components as well as the volatiles combustion characteristics are strongly influenced by the fuel mixture composition, which interferes with the electric field effects on the flame and heat energy production. With this account, the present study combines complex experimental study with mathematical modelling of the processes developing at the co-combustion of straw with peat pellets. Both the straw-to-peat mass ratio in the fuel mixture and the bias voltage of the axial electrode need to be varied to ensure the electric field applicability to control the main flame characteristics, to enhance the heat output from the device and to make the combustion emissions much cleaner.

2. Experimental

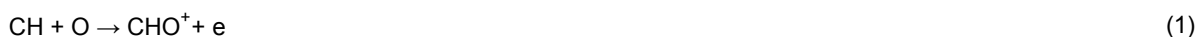
The electric field effects on the main flame characteristics and produced heat energy at the co-combustion of wheat straw and peat pellets were studied using a batch-size pilot device, which combines a biomass gasifier and the water-cooled sections of the combustor. The methodology of the experimental study of the electric field effects on the main flame characteristics is described in Barmina et al., 2016a. The gasifier was filled with a mixture of straw and peat pellets in various straw-to-peat mass ratios (from 100 % of peat to 100 % of straw). The thermal decomposition of the mixture was initiated and sustained up to 500 s by an external heat source of propane flame flow with the average heat power ≈ 1.3 kW. The gasification/combustion characteristics at the thermo-chemical conversion of the mixtures were studied experimentally at the average 1.6–1.7 air excess (α) in the flame reaction zone. The experimental study involved joint measurements of the main characteristics (elemental composition, heating values) of straw and its mixtures with peat pellets, measurements of the mixture weight loss rate (dm/dt), FTIR spectral analysis of the composition of volatiles at the combustor inlet (Zhao et al., 2017), calorimetric measurements of the heat output both from the gasifier and from the combustor, and flue gas composition analysis by the Testo 350. The ion density in the flame was measured using the double probe technique. The bias voltage of the axially inserted at the flame base electrode was varied in the range from 0 up to 2.4 kV. The ion current in the flame space was limited to 5–7 mA to avoid the formation of discharge. The elemental composition and heating values of wheat straw pellets, peat pellets and their mixtures in different proportions are summarized in Table 1.

Table 1: The elemental composition and heating values (HHV) of straw and peat pellets and their mixtures (dry mass)

Biomass	C, %	H, %	O, %	N, %	Moisture, %	Ash, %	HHV, MJ/kg
Wheat straw	46.62	5.09	42.72	1.31	9.10	4.26	18.50
Peat	53.83	5.12	36.93	1.11	11.40	3.02	21.20
Straw 10 % + peat	53.11	5.12	37.51	1.13	11.17	3.14	20.93
Straw 20 % + peat	52.39	5.11	38.09	1.15	10.94	3.27	20.39
Straw 30 % + peat	51.67	5.11	38.67	1.17	10.71	3.39	20.32

3. Experimental results and discussion

The electric field induced variations of the main flame characteristics at the co-combustion of straw and peat first of all depend on the formation of charged flame species, i.e. positive ions. Therefore, to provide the effective electric control of the main flame characteristics, it is necessary to apply the electric field to the flame area with a maximum of the ion concentration. It is generally accepted (Blades, 1975) that the formation of positive ions in hydrocarbon flames can be related to chemo-ionization reactions:



This suggests that the ion formation at thermal decomposition of biomass pellets is a consequence of the release of different traces of hydrocarbons (C_xH_y). The analysis of the produced gases released at the thermal decomposition of biomass pellets (straw, peat and their mixtures) confirms an intensive formation of the combustible volatiles (H_2 , CO) and hydrocarbon traces (C_2H_2 and CH_4), which are responsible for the formation of the flame reaction zone and primary flame ions (Figures 1a–d). The measurements of the radial and axial distributions of the flame ions have shown that the most intensive formation of the flame ions occurs at the primary stage of flaming combustion ($t < 1,200$ s). The peak value of the ion density ($5\text{--}6 \cdot 10^{17} \text{ m}^{-3}$) was observed at the bottom of the combustor ($L/D = 0.8\text{--}1$), close to the flame axis ($r/R = 0$), where the axial flow of hydrocarbon traces rapidly mixes with the air promoting the ion formation via the mechanism (1–3) (Figure 1d). Hence, to obtain the most intensive field-induced variations of the flame characteristics, the electric field must be applied to this part of the flame.

The experimental study of the field effect on the free flame shape and structure has shown, that with the given field configuration the electric field-induced body force (acting on the flame ions) promotes the reverse axial and radial heat/mass transfer of the neutral flame species (Barmina et al., 2016a) with apparent variations of the flame shape and length (Figures 2a–d).

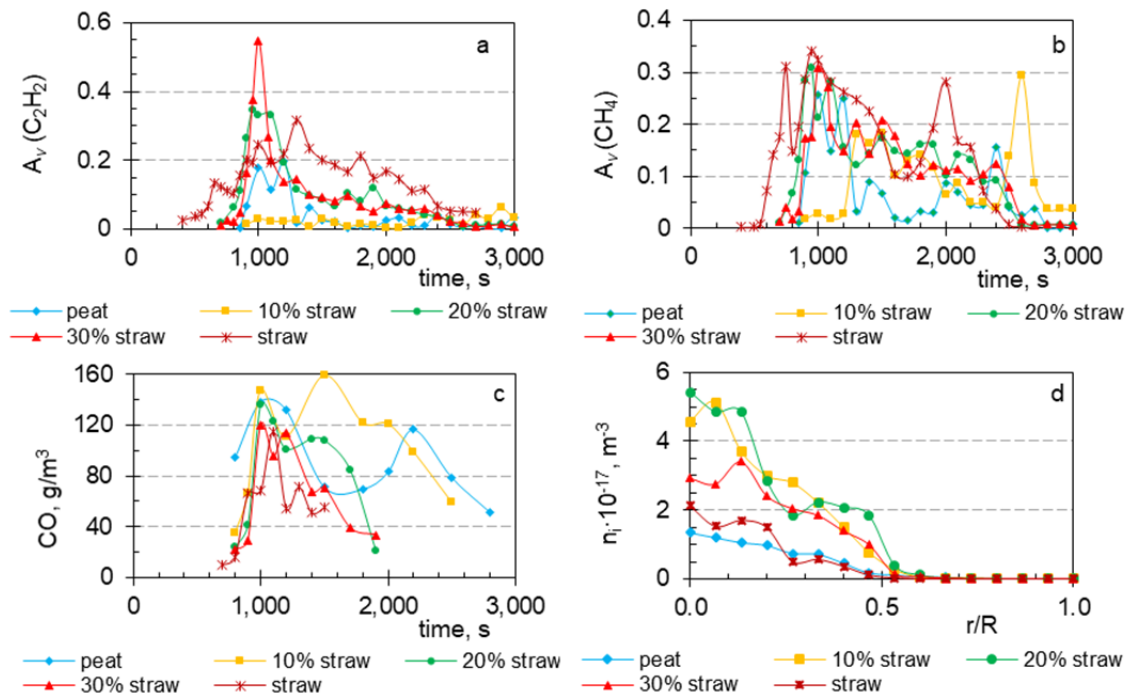


Figure 1: Effect of the mixture composition on the formation of hydrocarbon traces: C_2H_2 $\nu = 730\text{ cm}^{-1}$ (a), CH_4 $\nu = 3,017\text{ cm}^{-1}$ (b), combustible volatiles (c) and flame ions (d).

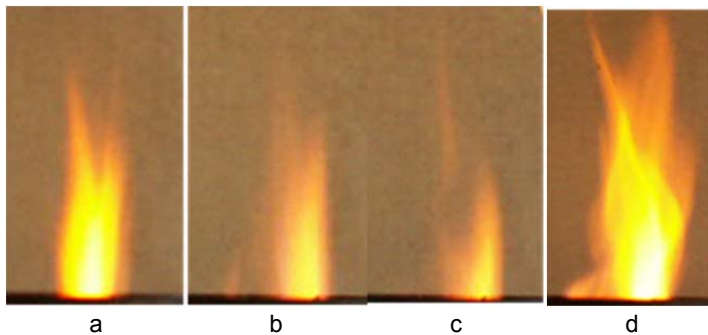


Figure 2: Effect of the variations of the bias voltage of the axial electrode on the free flame shape and length at thermo-chemical conversion of a straw-peat mixture: a – $U = 0$; b – $U = 0.6\text{ kV}$; c – $U = 1.2\text{ kV}$; d – $U = 1.8\text{ kV}$.

The field enhanced reverse axial heat transfer from the flame reaction zone down to the surface of the biomass pellets sustains the enhanced heating and thermo-chemical conversion of the pellets by increasing the weight loss rate of the biomass up to peak values (Figure 3a), the formation of which was observed at $U = 1.8\text{ kV}$ and started to decrease after $U > 1.8\text{ kV}$. The field-enhanced thermo-chemical conversion of the biomass mixture was confirmed by the increase of the CO_2 absorption intensity at the outlet of the gasifier ($CO_{2, \text{abs}}$) and by the increase of the average values of CO_2 volume fraction, which were estimated during complete burnout of the mixtures ($CO_{2, \text{sum}}$) and during combustion of volatiles ($CO_{2, \text{vol}}$) (Figure 3b), whereas the volume concentration of the volatiles (CO , H_2) at the outlet of the gasifier decreases to the minimum value (Figure 3c). This correlates with the increase of the heat output from the device (Figure 3d). The kinetic study of the gas flow composition at the outlet of the gasifier and combustor suggests that the most pronounced field-induced variations of biomass thermo-chemical conversion occur at the primary stage of the flame formation ($t < 1,200\text{ s}$). The field-enhanced ignition and combustion of the volatiles occurs at this stage, that result in rapid decrease of the volume concentration of the volatiles (CO , H_2) at the flame base with the correlating increase of the CO_2 volume fraction in the flue gas ($CO_{2, \text{vol}}$). At $U > 1.8\text{ kV}$ the field-enhanced reverse axial mass transfer of CO_2 towards the biomass surface balances the axial flow of volatiles and

advances the development of the endothermic process $C + CO_2 \rightarrow CO$, which leads to the decrease of the CO_2 volume fraction with the correlating increase of the CO mass fraction at the gasifier outlet (Figure 3c).

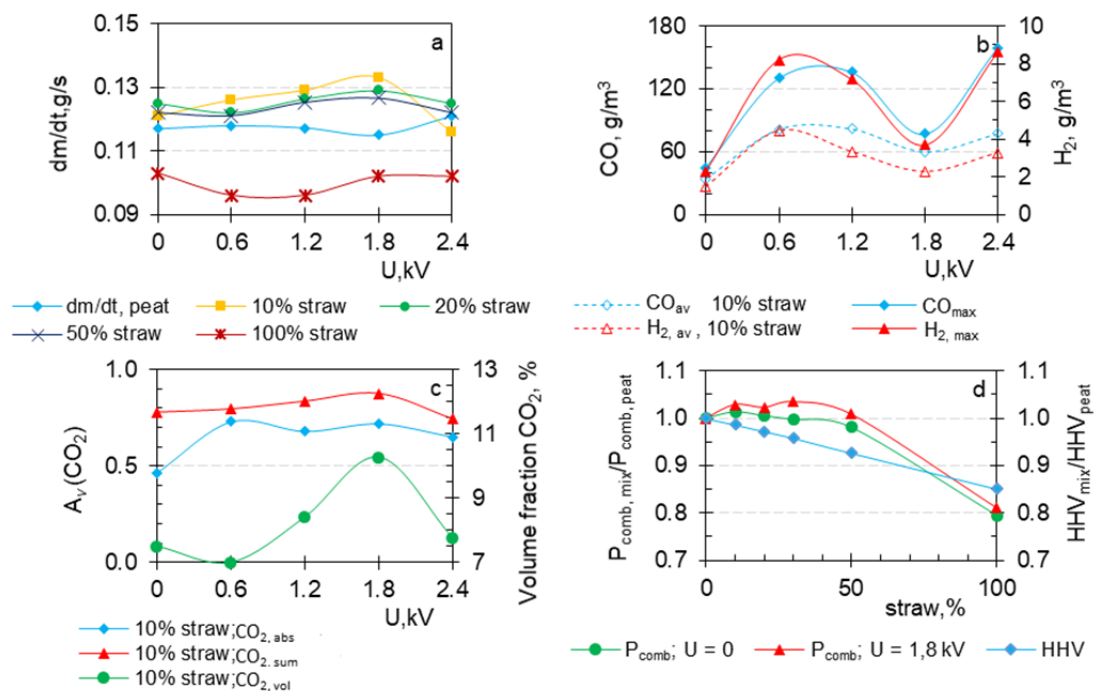
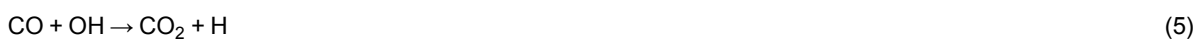


Figure 3: Electric field-enhanced variations of the weight loss rates (a), composition of volatiles (b), CO_2 absorption ($\nu = 668 \text{ cm}^{-1}$) at the gasifier outlet, CO_2 volume fraction in the flue gas (c), and of the heat output from the device (d).

Finally, it should be noted that from the results presented above (Figure 1, 3) it follows that the composition of the chemical substances released at the thermal decomposition of biomass pellets, the formation of the flame ions and the field impact on the flame during the co-combustion of straw with peat pellets strongly depend on the mass fraction of straw in the mixture. The peak value of the flame ions at the bottom of the combustor was observed at the average 10–20 % straw mass fraction in the mixture with the correlating increase of the electric field effect on the reverse axial heat mass transfer of the flame species (ion wind effect) promoting the field-enhanced thermal decomposition of the biomass mixture, the combustion of volatiles and the heat output from the device.

4. Results of mathematical modelling and numerical simulation of the electric field effects on the flame

For more detailed analysis of the processes developing downstream the combustor at the co-combustion of straw and peat pellets, the mathematical modelling and numerical simulation of the processes were performed using two dominant second-order chemical reactions of the volatiles (H_2 , CO) combustion:



The maximum values of the temperature, axial flow velocity and mass fractions of the CO_2 and H_2O species were obtained from the numerical analysis of the systems of 9 and 11 parabolic type partial differential equations (PDS). These describe thus the 1D compressible reacting swirling flow flame at the thermo-chemical conversion of pure straw/peat biomass pellets and during the co-combustion of 10–20 % of straw with peat. A numerical modelling was made in accordance with the experimental data assuming the CO and H_2 mass fractions as boundary conditions.

Studying the influence of the electric field on the thermo-chemical conversion of straw pellet in mixture with peat, a simplified model has been proposed considering the interplay of a 2D compressible axisymmetric flow

and the electrodynamical effects due to the Lorentz force's impact on flames in a cylindrical pipe (combustor) with radius $r_0 = 0.05$ m (Kalis et al., 2016). According to Barmina et al. (2017), the primary axial air flow and the oxidant were supplied with the bulk velocity $U_0 = 0.01$ m/s determining the axial velocity of the uniform flow in the central part of the combustor inlet. A simple exothermic chemical reaction $A \rightarrow B$ was simulated by Arrhenius kinetics using a single step reaction between the fuel and the oxidant. A more plausible model is the $A \rightarrow B \leftrightarrow C$ mechanism, where B represents the intermediate products and C the final products (Mikolaitis, 1987). This mechanism has been used for the investigation of the straw-peat (1:9 ratio) co-combustion, regarding the reactions between the chemical substances (CO , H_2 , O_2 , OH) and the formation of products (CO_2 , O , H_2O). The selected method helps to understand how the stationary flame is affected by the direct electric current between the axial electrode and combustor wall. The mathematical model of the reactions is described by the following three dimensionless reaction-diffusion equations in the cylindrical coordinates (r , $x = z/r_0$) at the time t :

$$\begin{cases} \frac{\partial T}{\partial t} + M(T) = P_1 \frac{1}{\rho} \Delta T + q_1 A_1 C_1 \exp\left(-\frac{\delta_1}{T}\right) + q_2 (A_2 C_2 \exp\left(-\frac{\delta_2}{T}\right) - A_3 C_3 \exp\left(-\frac{\delta_3}{T}\right)), \\ \frac{\partial C_1}{\partial t} + M(C_1) = P_2 \Delta C_1 - A_1 C_1 \exp\left(-\frac{\delta_1}{T}\right), \\ \frac{\partial C_2}{\partial t} + M(C_2) = P_2 \Delta C_2 + A_1 C_1 \exp\left(-\frac{\delta_1}{T}\right) - A_2 C_2 \exp\left(-\frac{\delta_2}{T}\right) + A_3 C_3 \exp\left(-\frac{\delta_3}{T}\right), \end{cases} \quad (8)$$

where

$$\Delta q = \frac{\partial^2 q}{\partial x^2} + \frac{1}{r} \frac{\partial}{\partial r} \left(r \frac{\partial q}{\partial r} \right), \quad M(q) = w \frac{\partial q}{\partial x} + u \frac{\partial q}{\partial r}, \quad q = T; C_1; C_2, \quad C_3 = 1 - C_1 - C_2, \quad (9)$$

C_1, C_2, C_3 are, respectively, the mass fractions of the reactant, the intermediate product and the final product; $w = u_z/U_0$, $u = u_r/U_0$ are the normalized axial and radial velocities; T is the normalized temperature in respect to the inlet temperature $T_0 = 300$ K; $P_2 = D/(U_0 \cdot r_0) = 0.01$, $P_1 = \lambda/(c_p \cdot \rho_0 \cdot U_0 \cdot r_0) = 0.05$, $q_1 = Q_1/(c_p \cdot T_0) = 5$, $q_2 = Q_2/(c_p \cdot T_0) = 1$, $Q_1 = 1.5 \cdot 10^6$ J/kg, $Q_2 = 0.3 \cdot 10^6$ J/kg are the heat losses for every reaction, $\delta_k = E_k/(R \cdot T_0)$, ($\delta_1 = \delta_3 = 10$, $\delta_2 = 13$) are the scaled activation energy; $R = 8.314$ J/(mol·K) is the universal gas constant; $E_1 = E_3 = 2.5 \cdot 10^5$ J/mol, $E_2 = 3.2 \cdot 10^5$ J/mol are the activation energies, $\lambda = 0.25$ J/(s·m·K) is the thermal conductivity, $D = 2.5 \cdot 10^{-4}$ m²/s is the molecular diffusivity of species; $A_k = A'_k \cdot r_0/U_0$, ($A_1 = A_3 = 5 \cdot 10^4$, $A_2 = 5 \cdot 10^5$) are the scaled pre-exponential factors ($A'_k = 1/\text{s}$); $c_p = 1,000$ J/(kg·K) is the specific heat capacity; ρ is the density normalized to the inlet density $\rho_0 = 1$ kg/m³, $k = 1; 2; 3$.

The meridian current densities j_r, j_z for the direct electric current (between the axially-symmetric electrode and the cylindrical combustor wall) are normalized to $j_0 = I/(2 \cdot \pi \cdot r_0^2)$ A/m², the azimuthal induction B_ϕ of the magnetic field – to $B_0 = \mu \cdot I/(2 \cdot \pi \cdot r_0)$ N/(A·m), the electromagnetic forces F_r, F_z j_r – to $F_0 = (j_0 \cdot B_0 \cdot N)/\text{m}^3$, where $\mu = (4 \cdot \pi \cdot 10^{-7})$ N/A² is the magnetic permeability and $I = 0(0.001)0.01$ A is the electric current.

The dimensionless radial and axial components of electromagnetic forces were quantified with the electromagnetic parameter $P_e = (B_0 \cdot j_0 \cdot r_0)/(\rho_0 \cdot U_0^2)$. For the dimensionless pressure p , the model of perfect gas $p = \rho \cdot T$ was used. The boundary conditions defined at Barmina et al. (2017) were adhered except for the ones of chemical species: along the axis $r = 0$ and at the wall $r = 1$, $\partial q/\partial r = 0$, at the outlet $x = 2$ - $\partial q/\partial x = 0$, at the inlet $x = 0$ - $C_2 = 0$ for $r \in [0; 1]$ and $C_1 = 1$ for $r \in [0; r_1]$; $C_1 = 0$ for $r > r_1$; $r_1 = 0.75$.

Table 2: Maximum values of the axial velocity (w_{max}), radial velocity (u_{max}), temperature (T_{max}), mass fraction of intermediate product ($C_{2, max}$), minimum value of the density (ρ_{min}), radial velocity (u_{min}), mass fraction of final product ($C_{3, min}$) and averaged value of the temperature (T_{av}) depending on the electromagnetic parameter P_e .

P_e	$C_{3, min}$	ρ_{min}	w_{max}/U_0	u_{max}/U_0	u_{min}/U_0	T_{max}/T_0	T_{av}/T_0	$C_{2, max}$
0	0.8022	0.033	4.58	2.61	0	3.650	3.376	0.4056
0.1	0.8025	0.036	4.59	2.62	-0.11	3.667	3.379	0.4062
0.2	0.8029	0.039	4.60	2.63	-0.25	3.693	3.384	0.4066
0.5	0.8037	0.052	4.81	2.66	-0.78	3.782	3.400	0.4066
1.0	0.8013	0.051	5.31	2.70	-1.73	3.910	3.398	0.4049
2.0	0.7850	0.048	6.67	2.74	-3.43	4.192	3.333	0.4025
2.5	0.7805	0.029	7.45	2.76	-4.14	4.290	3.296	0.4018

The distribution of the axial, radial and azimuthal components of velocity, density, and temperature has been calculated within the MATLAB package and summarized in Table 2. From these results one can see that for a mixture of peat and straw (10 %) pellets, the maximum value of the mass fraction of the intermediate product ($C_{2, \max}$), the minimum value of the mass fraction of the final product ($C_{3, \min}$) and the average temperature (T_{av}) increase at $P_e < 0.5$ and then decrease at $P_e > 0.5$ (a similar situation was observed for the maximum value of C_2 , i.e. at the gas outlet the maximum of $C_{2, \text{end}} = 1 - C_{3, \min}$). The maximum values of the temperature (T_{\max}), axial velocity (w_{\max}) and radial velocity (u_{\max}) increase with all values of P_e (the absolute values of the negative u_{\min} and vorticity also increase). The action of the electric body force at $P_e > 0.5$ leads to a reduction of the free flame length because of the decrease of the average temperature accompanied by the increase of the visible radius of the flame reaction zone at the inlet and by the increase of the flame temperature maximum.

5. Conclusions

With the aim to achieve a more effective use of straw as a fuel for energy production, the complex experimental study and mathematical modelling of the electric field effects on the processes developing downstream the combustor were performed. Both experimental and numerical data shows some comparable tendencies of the main straw-peat co-combustion flame characteristics varying the electric field force.

The results of present study reveal that the field effect on the main flame characteristics is determined by the mixture composition and by the formation of the flame ions. The maximum field effect achieved with ~10-20 % straw mass fraction in the fuel mixture when the field-enhanced reverse axial heat/mass transfer sustains the enhanced thermal decomposition of the biomass mixture. The enhanced thermal decomposition promotes an intensive release of the volatiles and their burnout, thus increasing the heat output from the device.

Acknowledgments

The authors would like to acknowledge financial support from the European Regional Development funding of project No.1.1.1.1/16/A/004.

References

- Barmina I., Kolmickovs A., Valdmanis R., Zake M., Kalis H., 2016b, Experimental and mathematical studies of electric field effects on biomass thermo-chemical conversion, *Chemical Engineering Transactions*, 50, 121-126. DOI: 10.3303/CET1650021., <www.aidic.it/cet/16/50/021.pdf>
- Barmina I., Purmalis M., Valdmanis R., Zake M., 2016a, Electrodynamic control of the combustion characteristics and heat energy production, *Combustion Science and Technology*, 188 (2), 190-206, <www.tandfonline.com/doi/full/10.1080/00102202.2015.10880>
- Barmina I., Valdmanis R., Zake M., Kalis H., 2017, The development of the gasification/combustion characteristics at thermo-chemical conversion of biomass mixtures, *Engineering for Rural Development*, 54-59, DOI: 10.22616/ERDev2017.16.N011, <www.tf.llu.lv/conference/proceedings2017/Papers/N011.pdf>
- Blades A.T., 1976, Ion formation in hydrocarbon flames, *Canadian Journal of Chemistry*, 54, 2919-2924.
- Hardy T., Musialik-Piotrowska A., Ciolek J., Mościcki K., Kordylewski W., 2012, Negative effects of biomass combustion and co-combustion in boilers, *Environment Protection Engineering*, 38, No. 1, 25-33.
- Kalis H., Barmina I., Zake M., Koliskins A., 2016, Mathematical modelling and experimental study of electrodynamic control of swirling combustion, *International Scientific Conference „Engineering for Rural Development”*, Jelgava, 134-141.
- Mikolaitis D.W. High temperature extinction of premixed flames. *Proceedings of the Conference Held in Juneau, Alaska, August 17-21, 1987 “Mathematical Modelling in Combustion Science”* Ed. J.D. Buckmaster, T. Takeno in *Lect. Notes in Physics* book series, 299, 67-77.
- Nordgren D., Hedman H., Padban N., Boström D., Öhman M., 2013, Ash transformation in pulverized fuel co-combustion of straw and woody biomass, *Fuel Processing Technology*, 105, 52-58.
- Olsson M., 2006, Wheat straw and peat for fuel pellets – organic compounds from combustion, *Biomass and Bioenergy*, 30, 555-564.
- Veijonen K., Vainikka P., Järvinen T., Alakangas E., 2003, Biomass co-firing an efficient way to reduce greenhouse gas emissions, *European Bioenergy Networks*, 1-26, <ec.europa.eu/energy/sites/ener/files/documents/2003_cofiring_eu_bionet.pdf>
- Zhao R., Yang N., Liu L., Duan R., Wang D., 2017, Characteristics of biomass gasification in flue gas by Thermo-Gravimetry–Fourier Transform Infrared spectrometer (TG–FTIR) analysis, *Chemical Engineering Transactions*, 61, 829-834. DOI: 10.3303/CET1761136., <www.aidic.it/cet/17/61/136.pdf>